Supporting Information

Balachandran et al. 10.1073/pnas.1106954108

SI Text

SI Methods ***Cell isolation and culture.*** Ovine tissues from animals weighing 20–25 kg and 8–10 mo of age were obtained under approved guidelines for animal experimentation at Children's Hospital, Boston. Primary cultures of mitral valve endothelial cells (MVECs) from ovine mitral valve leaflets were prepared and plated as single cells in 96-well plates as described previously (1–3). Briefly, clonal populations were isolated from MVECs at passage 2 by suspending in endothelial basal medium (EBM; Lonza), 10% heat-inactivated FBS (GIBCO), 1% L-glutamine-penicillin-streptomycin sulfate (GPS; GIBCO), and 2 ng/mL basic fibroblast growth factor (bFGF; Roche) at 3.3 cells per milliliter and plating 100 μL per well of a 96-well plate. When the colonies covered two-thirds of the well, cells were passaged into 24-well dishes. Cells were passaged 1:3 or 1:4 every 6–14 d and used between passages 6 and 14.

Microcontact printing and valve thin films. Fibronectin (BD Biosciences) was microcontact printed as described before (4) onto either regular elastomer stretcher membranes (Specialty Manufacturing, Inc.; 0.010" NRV) or onto valvular thin films (vTFs) in order to create either an isotropic or anisotropic tissue. For anisotropic tissue, fibronectin was microcontact printed in 20-μm-wide lines of 50 μg/mL concentration separated by 20-μm-wide gaps of 5 μg/mL concentration to provide cellular alignment cues. In isotropic tissue, fibronectin was microcontact printed with a flat polydimethylsiloxane (PDMS) stamp at 50 μg/mL concentration. Valvular thin films were constructed as outlined before (5) by spin-coating poly(*N*-isopropylacrylamide) (PIPAAm) (Polysciences) onto a prestretched elastomer membrane (SMI 0.010" NRV) then spin-coating PDMS (Sylgard 184) doped with 0.2-μm diameter fluorospheres (Invitrogen) on the PIPAAm. The construct was then cured at 65 °C for 4 h before being microcontact printed.

Cyclic stretcher experiments. MVECs were seeded on 5.5 × 8 cm elastomeric membranes within 20 cm^2 silicone reducer rings at a density of 25,000 cells per cm^2. A custom-built cyclic stretcher apparatus was used to subject samples to either 10% (Movie S1) or 20% strain (Movie S2) at 1 Hz, which is the normal resting heart rate of sheep. Stretching was started 30 min after seeding in order to allow the cells to form strong focal adhesions with the underlying substrate (Fig. S1). The device used a direct current motor (Maxon Precision Motors, Inc.) to displace the membrane a total of 5.5 mm (10% strain) or 11 mm (20% strain). Control samples were maintained unstretched (0% strain). The deformation was measured by marking the membrane with dots recording the deformation at 100 frames per second. The strain field of the membrane was then validated using an in-house three-point strain algorithm. We asked if cyclic stretch induced apoptosis and conducted a TUNEL assay of the stretched tissues, revealing no significant difference between conditions (Fig. S1*D*). Thus, our experimental model does not appear to be traumatic to the cells within the tissue.

Valve thin film contractile stress measurements. Valve thin film tissue stresses were calculated as previously published (5). Briefly, prior to the experiment, the tissues were cultured at 37 °C. At the time of the experiment, culture media was exchanged with Tyrode's buffer solution and the tissue and PDMS layers of the construct were cut into rectangular strips and the buffer was allowed to cool below 32 °C, dissolving the PIPAAm layer. The free-floating vTFs are then attached to polytetrafluoroethylene posts in a separate dish for stress measurement. The vTFs were maintained at 37 °C in a bath of Tyrode's solution. The vTFs were stimulated serially with 50 nM endothelin-1 (ET-1), 100 mM KCl, and 100 μM of the rho-kinase inhibitor HA-1077. The radius of curvature was measured under a stereomicroscope in both brightfield and fluorescence. The tissue stress was calculated by assuming that the vTF is a two-layered beam with one passive layer (PDMS) and one active layer (valve cells). The serial stimulation allows measurement of the basal contractile tone, or contraction stress prior to any stimulation, and the induced contraction or relaxation due to added compounds. The PDMS and tissue layer thickness needed to calculate vTF stress were measured using stylus profilometery (Dektak 6M; Veeco Instruments, Inc.) and confocal microscopy (Fig S3), respectively. Optimum concentration for ET-1 was based on dose curve experiments (Fig. S4).

Immunocytochemistry. After 48 h of culture, tissues were fixed in a solution of 4% paraformaldehyde (PFA) for 15 min and permeabilized with ice-cold methanol for 2 min. Samples were washed 3× with PBS solution (GIBCO) and then blocked using 1% BSA in PBS with 0.05% Tween-20 for 1 h at room temperature. Samples were then incubated with antibodies against α-smooth muscle actin (α-SMA, 1:1000; Sigma), phosphorylated-smad-2/3 (p-smad-2/3, 1:100; Santa-Cruz), β-catenin (1:500; Sigma), and VE-cadherin (1:25; Santa-Cruz) for 2 h at room temperature. Samples were subsequently washed 3× with PBS and then stained with appropriate secondary antibodies and DAPI (Sigma) for 1 h at room temperature, and coverslipped using Prolong Gold antifade reagent (Invitrogen). Confocal image stacks were captured with an LSM 510 Live (Zeiss) line scanning confocal microscope using a 40× objective.

Quantification of cell geometry parameters. After 24 h of culture, tissues were stained for their nuclei (DAPI), F-actin filaments (phalloidin), and cell membrane (VE-cadherin, 1:25; Santa-Cruz) as outlined above. Actin orientational order parameter (OOP) was calculated from phalloidin staining as previously published by us (6, 7). Briefly, the OOP was computed from the pixel-based orientation vectors of the actin images. The OOP was developed for the study of organization of liquid crystals (8) and adapted for biological applications (9). The parameter ranges from zero in isotropic systems to one in perfectly aligned systems. Nuclear eccentricity was calculated by thresholding the DAPI image, fitting an ellipse to each individual nucleus, and measuring the major and minor dimensions of the ellipse (10). Eccentricity is a measure of the shape of an ellipse and is in the range of [0,1]; a circle has an eccentricity of zero, and a more elongated shape is associated with a higher value of eccentricity. Cell aspect ratio and perimeter were also similarly calculated by fitting an ellipse to each individual cell around the border of the cell membrane, fitting an ellipse and calculating the ratio of major and minor lengths. A value of one corresponds to a circular shape, with larger values for cell aspect ratios indicating a more elongated shape. Phalloidin-stained images were also used for tissue thickness measurements (Fig. S4). Confocal stacks were first deconvolved (Fig. S4 *A* and *B*) using Imaris bitplane software (IMARIS) and an in-house MATLAB (Mathworks) code was used to calculate tissue thickness (Fig. S4 *C*–*E*). Tissue thickness data were utilized to calculate vTF contractile stresses (5). All geometric parameters were quantified based on at least 12 image

fields within a single tissue and from a total of at least four separate experimental runs.

Flow cytometry. Flow cytometry for VE-cadherin (1:20; Santa-Cruz) and α-SMA (1:100; Sigma) expressing cells was performed as described in Chaput et al. (11). Briefly, cells were trypsinized, fixed with 4% PFA for 10 min, and divided into two aliquots in order to stain the intracellular (α-SMA) and extracellular (VE-cadherin) protein separately. Cells were incubated for 24 h at 4 °C in primary antibody diluted in either PBS (extracellular) or 0.2% saponin/PBS (intracellular). Cells were washed 3× with PBS and incubated with appropriate secondary antibodies and imaged using a BD LSRII Flow Cytomter (BD Biosciences).

Western Blotting. After 48 h of culture, tissues were lysed in urea lysis buffer containing 100 mM Tris (pH 7.4), 4 M urea, 5 mM EDTA, 0.5% SDS, 0.5% Nonidet P-40, and protease inhibitor cocktail (Complete mini; Roche). Criterion 4–15% polyaccrylamide gels (Bio-Rad) were loaded with 10 μg of total protein and electrophoresed for 2 h at 0.04 A constant current. The gel was transferred to PVDF membranes for Western blotting analysis. Primary antibodies used were α-SMA (1:1000; Sigma), CD31 (1:200; Santa-Cruz), β-catenin (1:200; Santa-Cruz), TGF-β1 (1:100; AbdSerotec), smad-2 (1:300; Pierce), p-smad-2 (1:100; Pierce), and β-actin (1:5000; Santa-Cruz). Infrared conjugated secondary antibodies were used (1:10000; LICOR) and imaged with a LICOR Odyssey reader (LICOR). Quantification was performed by densitometry analysis using ImageJ (National Institutes of Health).

RNA isolation and quantitative real-time polymerase chain reaction. Total RNA was isolated using the Stratagene RNA isolation kit (Agilent Technologies). Reverse transcription was performed with iScript cDNA Synthesis Kit (Bio-Rad). Oligonucleotide primer sequences of interest are compiled in Table S1. PCR was performed with Ssofast Evagreen SuperMix (Bio-Rad) on a C1000 thermal cycler (Bio-Rad).

TGF-β1 inhibition experiments. A pharmacological inhibitor for the activin receptor-like kinase-4/5/7/smad-2 inhibitor 4-(5-benzo (1,3)dioxol-5-yl-4-pyridin-2-yl-1H-imidazol-2-yl) benzamide (SB-431542), was added to the culture medium at a concentration of 10 μM (12). Subsequent EMT was analyzed via analysis of α-SMA expression by Western blotting. The chosen SB-431542 concentration elicited maximum inhibition of EMT based on dose-response experiments (Fig. S3*B*). We also demonstrate efficacy of the inhibitor to inhibit TGF-β1 signaling via reduced expression of phosphorylated-smad-2 (Fig. S3*C*).

Statistical analyses. All data were first analyzed for normality using the Anderson–Darling method. All data except for nuclear eccentricity were normally distributed and subsequently analyzed by ANOVA as a function of tissue type (isotropic, anisotropic, or orthogonal) and strain magnitude followed by Tukey multiple pairwise comparisons. Nuclear eccentricity data were analyzed using the Mann–Whitney Rank Sum test. A p value of less than 0.05 was used to indicate statistical significance. All data are plotted as mean with error bars indicating standard errors.

1. Paranya G, et al. (2001) Aortic valve endothelial cells undergo transforming growth factor-beta-mediated and non-transforming growth factor-beta-mediated transdifferentiation in vitro. *Am J Pathol* 159:1335–1343.
2. Paruchuri S, et al. (2006) Human pulmonary valve progenitor cells exhibit endothelial/mesenchymal plasticity in response to vascular endothelial growth factor-A and transforming growth factor-beta2. *Circ Res* 99:861–869.
3. Wylie-Sears J, Aikawa E, Levine RA, Yang JH, Bischoff J (2011) Mitral valve endothelial cells with osteogenic differentiation potential. *Arterioscler Thromb Vasc Biol* 31:598–607
4. Feinberg AW, et al. (2007) Muscular thin films for building actuators and powering devices. *Science* 317:1366–1370.
5. Alford PW, Feinberg AW, Sheehy SP, Parker KK (2010) Biohybrid thin films for measuring contractility in engineered cardiovascular muscle. *Biomaterials* 31:3613–3621.
6. Bray MA, Sheehy SP, Parker KK (2008) Sarcomere alignment is regulated by myocyte shape. *Cell Motil Cytoskeleton* 65:641–651.
7. Grosberg A, et al. (2011) Self-organization of muscle cell structure and function. *PLoS Comput Biol* 7:e1001088.
8. Hamley IW (2007) *Introduction to Soft Matter : Synthetic and Biological Self-Assembling Materials* (Wiley, Hoboken, NJ), Rev. Ed, pp 18–19.
9. Volfson D, Cookson S, Hasty J, Tsimring LS (2008) Biomechanical ordering of dense cell populations. *Proc Natl Acad Sci USA* 105:15346–15351.
10. Bray MA, et al. (2010) Nuclear morphology and deformation in engineered cardiac myocytes and tissues. *Biomaterials* 31:5143–5150.
11. Chaput M, et al. (2009) Mitral leaflet adaptation to ventricular remodeling: Prospective changes in a model of ischemic mitral regurgitation. *Circulation* 120(Suppl 11): S99–103.
12. Ruiz E, Redondo S, Gordillo-Moscoso A, Tejerina T (2007) Pioglitazone induces apoptosis in human vascular smooth muscle cells from diabetic patients involving the transforming growth factor-beta/activin receptor-like kinase-4/5/7/Smad2 signaling pathway. *J Pharmacol Exp Ther* 321:431–438.

Fig. S1. Representative time series images (*A*) of VECs being seeded on elastomeric membranes to yield isotropic (*Upper*) or anisotropic (*Lower*) tissues. Cells start to form adhesions to the underlying fibronectin within 10 min and form confluent tissue within 30 min of initial seeding. (Scale bar: 100 μm.) Stretching protocol begins at this point. VEC tissues are subject to one of eight different cyclic strain protocols for 24 or 48 h before being analyzed (*B*). Representative fluorescent images (*C*) of subconfluent isotropic and anisotropic VEC tissues showing fibronectin (*C*, *i* and *iii*) and nuclear and actin stains (*C*, *ii* and *iv*). For the isotropic tissues, note region in top left of *C*, *i* showing uniform, isotropic coating of fibronectin where cells are absent. Also note robust alignment of VECs to cues from fibronectin lines in *C*, *ii* and *iv*. (Scale bar: 50 μm.) Cyclic strain treatment did not induce increased tissue damage as determined via TUNEL cellular apoptosis assay, compared to controls (*D*) ($n = 4$).

Fig. S2. Quantification method for cell morphological parameters. Representative DAPI and phalloidin-stained VEC tissues (*A*) were analyzed for both actin orientation and nuclear eccentricity. We first use fingerprint detection algorithms to obtain an actin vector map and a histogram of actin orientation angles over each image field. This histogram of the orientation angles of these actin vectors is then compiled and cumulated over all image fields to yield the actin orientation order parameter. The DAPI image of the same fluorescently stained VEC tissue is then thresholded and nuclei are outlined. Nuclear eccentricity was then calculated by fitting an ellipse to the thresholded nuclei. Cell aspect ratio (*B*) is measured by first thresholding VE-cadherin stained tissues (*C*), outlining the cell borders, fitting an ellipse to the cell border, and plotting the ratio between major and minor axis lengths. (Scale bar: 25 μm.) Graphs, mean ± SEM; $n = 6$; $^*p < 0.05$.

Fig. S3. Immunofluorescent staining of 10% anisotropic tissues revealed punctate p-smad-2/3 nuclear expression (*Inset*, white) in cells that were also positive for α-SMA (*Inset*, green), suggesting EMT potentiated by TGF-β signaling (*A*). (Scale bar: 50 μm.) Concentration-response curve of the TGF-β1 inhibitor SB-431542 on anisotropic VECs stretched to 10% was used to choose 10 μM as the concentration for inhibition experiments (*B*). Graphs, mean ± SEM; $n = 4$. The inhibitor SB-431542 inhibited TGF-β/smad-2 signaling in both 10% and 20% strain groups as demonstrated by down-regulation of phosphorylated-smad-2 expression (p-smad-2). Smad-2 expression was used as controls (*C*).

Fig. S4. Tissue thickness was measured based on F-actin immunostaining and was a required input for calculating valve contractility. Confocal images were first deconvolved to reverse the effects of optical distortion from the microscope. An in-house MATLAB code was utilized to calculate the mean thickness of tissues. Representative deconvolved and rendered confocal images of isotropic (*A*) and anisotropic (*B*) VEC tissue. (Scale bar: 20 μm.) Representative thickness heat maps of isotropic (*C*) and anisotropic (*D*) tissues demonstrating regions of increased peak tissue thicknesses in anisotropic tissue compared to isotropic tissues. Mean tissue thicknesses (*E*) reported for the different treatment groups. Graphs, mean ± SEM; $n = 4$; $*p < 0.05$.

Fig. S5. Concentration-response curve of the endothelium-derived vasoactive mediator ET-1 on valve interstitial cells (VICs) was used to choose 50 nM as the concentration for thin film experiments (*A*). An anisotropic monolayer of pure VICs were seeded on the vTF and used for the ET-1 concentration response. Total contractile stress developed in transformed VEC samples after exposure to ET-1 and KCl. Contractile stress in samples stretched to 10% and 20% strain was significantly greater than control (*B*). All graphs, mean ± SEM; $n = 8$; $*p < 0.05$.

Movie S1. Representative video showing stretchers on our cyclic stretcher device subject to 10% strain.

Movie S1 (AVI)

Movie S2. Representative video showing stretchers on our cyclic stretcher device subject to 20% strain.
Movie S2 (AVI)

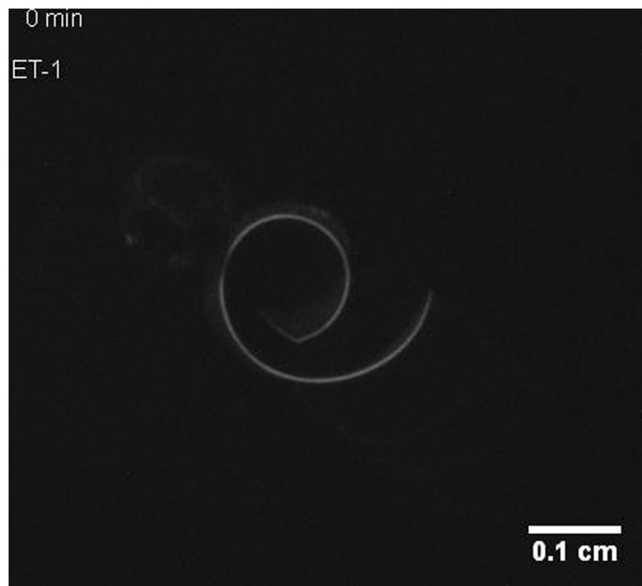

Movie S3. Representative vTF during serial stimulation with 50 nM ET-1, 100 mM KCl, and 100 μM HA-1077.
Movie S3 (AVI)

Table S1. List of gene primers used in this study.

Gene name	Forward primer (5′-3′)	Reverse primer (5′-3′)
TGF-β1	TAACACGCTTCAAGTGGACA	TCCGGAAGTCAATGTAGAGC
WNT1	CAGCATAGAGCCGGGCAAG	AGGAGAGTGCTCCCTGGGGC
VEGF	ATTTTCAAGCCGTCCTGTGT	CCTCGGCTTGTCACATTTTT
ACTB	CAAGGAGAAGCTCTGCTACG	TAGAGGTCTTTGCGGATGTC